Correlating the compliance and permeability of photocrosslinked polyelectrolyte multilayers

Ali M. Lehaf, **Maroun D. Moussallem**, and **Joseph B. Schlenoff**

Department of Chemistry and Biochemistry The Florida State University Tallahassee, Florida 32306

Abstract

Photocrosslinkable polyelectrolyte multilayers were made from poly(allylamine), PAH and poly(acrylic acid), PAA, modified with a photosensitive benzophenone. Nanoindentation, using atomic force microscopy, AFM, of these and unmodified PAH/PAA multilayers was used to assess their mechanical properties *in situ* under aqueous buffer. Under the conditions employed (and a 20 nm AFM radius tip) reliable nanoindentations that appeared to be decoupled from the properties of the silicon substrate were obtained for films greater than 150 nm in thickness. A strong difference in apparent modulus was observed for films terminated with positive as compared to negative polyelectrolyte. Films terminated with PAA were more glassy, suggesting better charge matching of polyelectrolytes. Multilayers irradiated up to 100 minutes showed a smooth and controlled increase in modulus, with little change in water contact angle. The permeability to iodide ion, measured electrochemically, also decreased in a controlled fashion

Keywords

photocrosslinking; force spectroscopy; final layer effect; Young's modulus; permeability

Introduction

Among the applications of polyelectrolyte multilayers, PEMUs, modification of the biological interface is gaining much attention.[1] For example, the mechanical properties of the cellular microenvironment affect cell motility, adhesion, protein and gene expression and differentiation.[2] Cells generally adhere and spread better on stiff substrates[3-6] and they migrate from the soft part of the substrate to the stiff part in a process known as "durotaxis" when plated on surfaces with gradient elasticity.[4,6,7] Substrate stiffness was also shown to influence cell differentiation.[2,8,9]

Because the modulus of a polymer thin film is convoluted with that of the substrate, the measured or effective modulus of a PEMU depends on how the measurement is made and the film thickness. Theoretical treatments for cells adhering to PEMUs have demonstrated a strong dependence on thickness for the modulus sensed by a cell.[10,11] The bulk modulus of a PEMU depends on the density of ion pair crosslinks between positive and negative polyelectrolyte chains.[12] This physical crosslink density may be controlled, in turn, by adding a salt to the solution, which breaks ion pairs. Clearly, this is not a valid approach for

physiological systems, where the ionic strength must remain within a narrow window. Thus, more classical methods of chemical crosslinking have been employed in PEMUs. For one system used extensively to make multilayers, poly(allylamine), PAH, and poly(acrylic acid), PAA, the amine and carboxylate functional groups condense under heating to yield extensive amide crosslinks.[13,14] The same functional groups also undergo coupling under ambient, aqueous conditions using well-known coupling agent, such as carbodiimides (EDC),[15] glutaraldehyde,[16] or anhydride reagents.[17]

Photo crosslinking offers precise, room temperature control over crosslinking density without the use of reagents that may be toxic to cells.[18] Photo crosslinking, which may be performed in vitro or in vivo,[19] is particularly effective when the crosslinking moiety is built into the backbone of one of the polyelectrolytes.[20] Furthermore, photo crosslinking offers the possibility of photopatterning areas of a multilayer with resolution that is not achieved by thermal or chemical crosslinking.[21] Several recent publications describe the use of photo crosslinking in PEMUs.[18,22-26]

The earliest work on chemically crosslinked PEMUs focused on the control of permeability through multilayers. Ion transport, for example, was shown to significantly decrease on thermal crosslinking,[27] with a concomitant increase in charge selectivity.[20,28] More recent interest in crosslinking is motivated by the ability to modify the release rate of drugs and other bioactive molecules from PEMU capsules and films.[23] Permeability and mechanical properties of water-swollen systems like PEMUs are expected to be somewhat related, as softer, more hydrated materials also tend to be more permeable. However, we have shown that for ion transport through PEMUs, membrane ion content controls transport.[29] Both thermal crosslinking and chemical crosslinking of PEMUs with, for example, carboxylates and amines, reduces the total ion content, whereas the benzophenone photochemistry described here preserves the net charge within a PEMU. We were interested in measuring ion permeability of PEMUs as a function of crosslinking and correlating changes to mechanical properties.

The fact that PEMUs are thin films makes measuring their mechanical properties more challenging. Nanoindentation measurements may be employed to measure the apparent modulus of relatively thin samples.[18,30-34] Elastic response, as a result of the loading force, can then be analyzed.[35] The quartz crystal microbalance (QCM) is useful for measuring the high-frequency response of relatively thick PEMUs.[36] We were able to perform more traditional tensile testing, including frequency dependent response, on thick, free-standing PEMUs.[12,37]

In this paper we explore a polyelectrolyte multilayer made from PAH and PAA modified with benzophenone, which allows photocrosslinking without changing the density of charge within the PEMU. The Young's modulus of the PEMU following UV irradiation was determined by nanoindentation (using an atomic force microscope). The degree of crosslinking and stiffness were then correlated with ion permeability under tight control of the crosslinking density.

Materials and Methods

Poly(acrylic acid) (PAA M_w = 100,000 g/mol) and poly(allylamine hydrochloride) (PAH M_w = 56,000 g/mol) were used as received from Aldrich. NaCl (ACS grade) was used to adjust the ionic strength of the polyelectrolyte solutions. Poly(ethyleneimine) (PEI Mw = 70,000 g/mol) obtained from Polysciences. Potassium iodide (ACS reagent) from Aldrich was used for the permeability studies. 4-hydroxybenzophenone from AlfaAesar, potassium carbonate anhydrous from Fisher Scientific and 2-bromoethanol from Acros Organic were

used in the synthesis of the photocrosslinker. N,N'-dicyclohexylcarbodiimide (DCC) from Fluka was used for coupling PAA to benzophenone.

Synthesis of 4-(2-hydroxyethoxy)benzophenone (1)

3.96g of 4-hydroxybenzophenone (16 mmol) was dissolved in 24 mL of acetone, to which 5.6g of K_2CO_3 (40 mmol) was added. The mixture was stirred under reflux for 30 min. 5.46 g of 2-bromoethanol (44 mmol) was added dropwise to the reaction mixture and the reaction was left to stir for 10 h. After the reaction mixture was cooled to r.t.16 mL of water was added and the product extracted with diethylether. Diethylether was removed under reduced pressure, and the product recrystallized from ethanol giving white crystals. Yield = 40%. ^{1}H NMR (CDCl$_3$, 300 MHz, δ in ppm) (Figure S1): 7.82-7.84(d,2H) ,7.75-7.77(d,3H), 7.46-7.60(m,2H), 6.98-7(d,2H), 4.16-4.19(t,2H), 3.99-4.04(m,2H), 2-2.04(t,1H).

Synthesis of poly(acrylic acid) "PAA" grafted with of 4-(2-hydroxyethoxy)benzophenone (Bp) "PAABp"

3.42g (47 mmol) of PAA was dissolved in 90 mL of anhydrous dimethylformamide (DMF), then 2.87g (11 mmol) of 4-(2-hydroxyethoxy)benzophenone was added to the solution and the mixture stirred for 10 min at 65 °C. 1.95 g of dicyclohexylcarbodiimide (9.48 mmol) was added and the reaction mixture was heated for 12 h at 65 °C under stirring. The reaction was cooled and the white crystals of dicyclohexyl urea were removed under centrifuge. The mixture was concentrated under reduced pressure and 5 mL of DMF was added to the residue which leads to the formation of more urea crystals which were also centrifuged out. The product was precipitated in ethyl acetate to give white crystals of PAA grafted with benzophenone "PAABp". The grafting percent, determined from a UV-Vis calibration curve, was found to be 5 mol%. ^{1}H NMR (DMSO, 300 MHz, δ in ppm) (Figure S2): 7.694 (br m), 7.531 (br m), 7.091 (br m), 4.275 (br m), 2.204 (br s), 1.731 (br s), 1.469 (br, s).

Polyelectrolyte multilayer (PEMU) buildup

PAH/PAABp multilayers were built with the aid of a robot (StratoSequence V, nanoStrata Inc.) on a 1 inch diameter single side polished silicon wafer for AFM measurements and on fused silica slides for UV-Vis measurements. The substrates were cleaned in piranha (70% H_2SO_4 and 30% H_2O_2) for 20 minutes (caution: piranha is a strong oxidizer and should not be stored in closed containers) and then rinsed vigorously with distilled water (18 M) and dried with N_2. Each of the polymer solutions were 10 mM (with respect to the repeat unit) in Tris buffer at pH 7.4. The ionic strength of the polymer solutions was adjusted to 150 mM using NaCl. Surfaces were primed with a layer of PEI by dipping into PEI solution for 30 minutes, and then rinsed with water. The substrate was mounted on a shaft that rotated at 300 rpm. The dipping time in each of the polymer solutions was 5 min followed by three 1 min rinsing steps in water. PEI(A/B)$_x$ and PEI(A/B)$_x$A indicate a multilayer ending in B and A respectively, where A represents the polyanion and B the polycation.

The dry thickness of the PEMU film was obtained by using a Gaertner Scientific L116S autogain variable angle Stokes ellipsometer unless stated otherwise. Ten thickness measurements on each PEMU were averaged.

Static contact angle was used to measure the effect of photocrosslinking on the wettability of PAH/PAABp multilayer at different irradiation times. The static contact angle was determined using a KSV Cam 200. The volume of water droplet was 10 μl for all measurements and each measurement point was an average of 3 points taken at different locations on the PEMU.

PAH/PAABp crosslinking

The PEMU was irradiated a dry state in a CL-1000 Model 254 nm UV box (Ultra-Violet Products Ltd. , wavelength range 200 - 280 nm) equipped with a calibration photodiode. The UV crosslinker consisted of 5 UV lamps (8 W each) having dimensions of $12.70 \times 30.5 \times 25.4$ cm. Samples were placed at the center of the box. The UV intensity at the sample was 4.9 mW cm^{-2}

The efficiency of crosslinking was studied using a Cary 100 Bio UV-Visible spectrophotometer. UV-Vis measurements were performed on a multilayer built on a fused silica slide to monitor the absorption of benzophenone unit following different irradiation times.

Force spectroscopy

Force indentation measurements, or force curves, were obtained using an AFM,[38] as described by Moussallem et al..[33] An MFP-3D AFM unit was equipped with an ARC2 controller (Asylum Research Inc., Santa Barbara, CA) and Igor Pro software. AC240-TS tips with a spring constant of ~2 N m^{-1} were used for indentation. After calibrating the optical lever sensitivity (OLP) of the tip, the spring constant was calibrated in air using the thermal fluctuation technique. The tip was immersed in the buffer solution and the OLP recalibrated. Force maps of 4 x 5 were performed on the bare silicon wafer where the tip was recalibrated and then on the PEMU with a scan size of 20×20 μm. All force maps were performed *in situ* with the sample immersed in Tris buffer at pH= 7.4 and in 0.15 M NaCl. The distance from the surface and the velocity of the tip was set to 500 nm and 1μm s^{-1} respectively.

The force applied, which deflects the cantilever, and the resulting indentation are given by:

$$\delta = (z - d) \tag{1}$$

$$F_{applied} = Kd = K(z - \delta) \tag{2}$$

where δ is the indentation of the tip into the material, z is the distance of the tip relative to the material in the z-direction, d is the deflection of the tip, and K is the spring constant of the cantilever.[33] Force curves are analyzed based on tip geometry,[38] using Hertzian contact mechanics that provide solutions to the indentation of a semifinite substrate with a hard probe.[33] In this paper, force curve analysis was based on Sneddon's model, that describes a conical tip[39] where force vs. indentation is represented by Equation 3.

$$F_{cone} = \frac{2E_{surface}}{\pi \left(1 - \upsilon^2_{surface}\right)} \tan(\alpha)(z - d)^2 \tag{3}$$

and a punch model represented in Equation (4).[32,33,40]

$$F_{punch} = 2\frac{E}{(1 - \upsilon^2)}R(z - d) \tag{4}$$

where E is the modulus of the material, R is the radius of the indenter, υ is the Poisson ratio of the material, and α is the half angle of the tip.[32,33]

Force *vs*. indentation for uncrosslinked films were quadratic thus a cone fit was used to obtain the Young's modulus. For crosslinked films a linear dependence of force on indentation was obtained and thus a punch model was used. The apparent modulus, E_a, can be related to Young's modulus of the indented material and the indenter using Equation 5.[34] Force *vs*. indentation graphs were fitted up to 20 % indentation in order to minimize effects of the substrate on measured sample stiffness. The half angle and the radius of the tip were 18° and 10 nm respectively (provided by the manufacturer).

$$E_a = \left(\frac{1 - v_1^2}{E_1} + \frac{1 - v_2^2}{E_2} \right)^{-1}$$

(5)

E_a is the apparent modulus, E_1 and v_1 are the Young's modulus and Poisson ratio of the indented material respectively, E_2 and v_2 are the Young's modulus and Poisson ratio of the silicon indenter. The value for E_2 was set to 150 GPa and the of v_2 was set to 0.27. The value for v_1 was set to 0.5 as the PEMUs were considered as to be isotropic elastic materials in the range of loads applied.[33]

Images of the surface topology were obtained using the same equipment in scanning mode .AC mode was used for dry images and contact mode for wet images to obtain the morphology of the surface. The scan size was set to 20×20 μm and the scan rate was 0.5Hz. Thickness measurements were determined by scratching the film with a tweezers, and then scanning a 90×90 μm area over the scratch. The thickness was measured by drawing a line ,using Igor sodtware, across the scratch and the height of the film was obtained, the height was obtained at different positions of the image and the average height was reported. The rms roughness of the image was obtained by using a 1×1 μm square patch and determined by the software, ten values were recorded at different positions of the image and the average value was reported.

The FTIR data was obtained using a nitrogen purged FTIR (Nicolet Nexus 470 with a DTGS detector) spectrometer. The resolution was 4 cm^{-1} and 256 scans were taken on the sample. The samples were held at 15° off perpendicular to avoid interference fringes

Permeability of Iodide ion at different irradiation times

A 100 mL electrochemical cell equipped with a temperature controlled water jacket was filled with approximately 50 mL 0.15 M NaCl and 1 mM KI. The counter electrode was platinum foil, and the reference a KCl saturated calomel electrode, against which all potentials were quoted. The working electrode was a 5 mm diameter rotating platinum disk (RDE, from Pine Instruments) mounted in a Pine AFMSRCE rotator and speed controller. Linear potential ramps were generated with the aid of Pine AFCBP1 potentiostat and the resulting voltammograms were recorded using Aftermath software. Before coating the electrode with PAH/PAABp multilayer, the electrode was polished with 0.05 μm alumina, sonicated, and then rinsed with water. The electrode was then coated with PEI(PAABp/PAH)$_{15}$ as described above.

Results and Discussion

Effect of thickness and final layer on the Young's modulus

Three variables were probed during the buildup of PAH/PAA multilayers. The first was film thickness as a function of layer number. The second was the apparent or measured modulus as a function of film thickness, and the third was the modulus as a function of whether the PEMU was terminated with PAH or with PAA. Even/odd pairs were measured every 3

layers i.e. 14, 15, 18, 19, 22, 23, 26, 27, 30, 31, 34, 35, 38, 39. Thickness and force curve measurements were obtained (Figure 1) where the thickness was measured as dry. Dry thickness as measured by the ellipsometer is presented in Figure 1 because it was more accurate (+/- 3%) and force curves were performed *in situ* in saline buffer (Tris buffer at pH= 7.4 with 0.15 M NaCl). The wet thickness of PEMUs can be obtained from the dry thickness using the index of hydrobicity[41] which is the ratio of the wet to dry thickness of the multilayer. The index of hydrobicity for PAH/PAA and PAH/PAABp were measured using an AFM. PEMUs on silicon wafers were scratched and the thickness determined at step edges before and after immersion in saline buffer (pH=7.4, 0.15 M NaCl) .Respective indices of hydration were 1.22 and 1.29. It was found that about 14 layers were required (under the conditions employed) to obtain linearly growing films with reproducible modulus measurements, corresponding to a minimum wet thickness of about 60 nm. While measurements were possible, apparent modulus values did not stabilize until a wet thickness of about 180 nm was achieved (>25 layers). Decreasing apparent modulii before this point, and stabilization afterwards, were interpreted as a contribution of the substrate (silicon) to the apparent modulus for thinner films.

We were surprised to see a strong dependence of apparent modulus on the terminating layer, in contrast with the nanoindentation results of Thompson et al.[42] who found no dependence of compliance of the final layer for a PAH/PAA multilayer. In Figure 1, the modulus of a PAH terminated film is about one third that of a PAA terminated one. The finding that the PAA-terminated films were stiffer was also unexpected. PAA is a hydrophilic polymer that makes swellable, less strongly-bound multilayers which can be decomposed with an increase in salt concentration[43] or a change in pH.[44] In contrast, PAH makes less hydrated, more resilient (e.g. harder to swell) PEMUs.[45,46] With sufficient thickness (Figure 1) the modulus oscillates between about 70 MPa for PEMUs ending in PAA and about 20 MPa for those ending in PAH. This final layer effect was not seen for highly hydrated "exponentially" grown PEMUS, such as PLL/HA.[30,31]

Last-layer effects have been observed widely in PEMUs. For example, ion permeability depends on the last layer.[47,49] Water content (measured by NMR),[50,51] or IR[45] is also a strong function of the identity of the last layer. Figure 1 shows clear evidence for a more glassy surface when terminated by PAA. The properties of individual, dry polyelectrolytes are quite different when they are hydrated or part of a complex. The stoichiometry of polyelectrolyte complexes strongly controls modulus. For example, a multilayer that contains a large amount of extrinsic charge (i.e. counterions) has a significantly lower modulus.[12] If high modulus is associated with good charge matching of polyelectrolytes, it follows that the PEMU surface terminated with PAA must be more intrinsically compensated than one terminated by PAH. If extrinsic compensation is caused by polymer diffusion, the diffusion range of PAA into the PEMU is less than that of PAH. An alternative view of the morphology of the PEMU surface is that it consists of a sharply-terminated blend of PAA and PAH and a highly diffuse layer of pure PAA which has such a low modulus that it cannot be measured with the tip used for Figure 1. We are currently exploring this possibility.

The effect of substrate when doing force curves was studied in a separate experiment. Two multilayers were compared, one of 23 layers with a wet thickness of 146 nm, and one of 31 layers (262 nm), where both multilayers had PAH as the final layer. Force curves were performed on both multilayers immersed in Tris buffer at pH= 7.4 and 0.15 M NaCl and the resulting force *vs*. indentation profile were fitted at indentation distances from 0 to 10 nm, then 10 to 20 nm then 20 to 30 nm and up to the highest indentation (see Figure 2) . For the thinner PEMU, the effective modulus remained constant up to about 1/3 the thickness (49 nm) at which point the modulus of the substrate started to be convoluted with that of the

multilayer. This observation places the lower limit for reliable indentation of a PEMU using a 20 nm diameter tip at about 100 nm. Sharper tips would probably show steady-state values for thinner PEMUs. For the thicker multilayer the modulus remained constant throughout the indentations tested.

PAH/PAABp multilayer and photocrosslinking

There have been several approaches to improving the stability and mechanical properties of polyelectrolyte multilayer, particularly under varying pH and/or ionic strength.[41,42] The most common way to enhance the stability and stiffness of polyelectrolyte multilayer is by converting the weak ion pairing interactions that hold the multilayer together into covalent bonds. This can be achieved by chemical crosslinking groups such as amines and carboxylic acids to form amide bonds,[30] or by thermally crosslinking these groups,[14,33] or by photocrosslinking, which involves the introduction of a photocrosslinkable moiety into the multilayer.[18,20,22,52,53]

Benzophenone, a light absorbing component, serves as a free radical source suitable for photocrosslinking. Excited benzophenone (n,π* electronic transition) has a biradical that is able to abstract hydrogen from its surrounding,[54,55] which, leads to crosslinking by the formation of C-C bond,[54,56] PAA grafted with a benzophenone molecule was synthesized, following the method of Park et al.,[20] to effect photocrosslinking as shown in Scheme 2. Because the Bp side chain linker arm is shorter than that used by Park et al. the crosslinking is expected to yield stiffer material.

The percentage of benzophenone on PAA was obtained from a calibration curve of benzophenone dissolved in dimethyl formamide (DMF) and by performing UV-Vis measurements of absorption vs. concentration of benzophenone (Figure S6). The grafting degree of benzophenone on PAA was found to be 5 mol % (i.e. the maximum crosslink density possible is 5 mol %) and this was used as a polyanion to build a multilayer with PAH as the polycation. The multilayer was prepared on a fused silica slide and irradiated with UV. Benzophenone absorbs UV and, in the excited state, is able to abstract hydrogen from its surroundings, leading to the formation of ketyl radical, which forms a C-C bond with the polymer, or the excited benzophenone can return to the ground state by phosphorescence.[57] Figure 3 shows the decrease in the absorption peak of benzophenone with irradiation time as a result of the loss of the carbonyl group, The extent of crosslinking given as the percentage of crosslinked benzophenone of PEI(PAABp/PAH)$_{15}$, was obtained using Equation 6.

$$\%Bp_{crosslinked} = \frac{(A_o - A_t)}{A_0} \times 100$$

(6)

Where $\%Bp_{crosslinked}$ is the percentage of crosslinked Bp within the multilayer, A_0 is the initial absorption of Bp before irradiation, and A_t is the absorption of Bp after irradiation for a given time t. The crosslinking was most efficient during the first 30 seconds where benzophenone molecules were more available. As irradiation time was increased the crosslinking rate became slower, since the multilayer was becoming more compact and chains less mobile, making it more difficult to crosslink the other benzophenone molecules. After 100 mins of irradiation 20% benzophenone remained uncrosslinked see Figure 3.

The chemical transformation depicted in Scheme 2 was verified with IR spectroscopy measurements on a multilayer coated on a double-side polished silicon wafer. For this particular measurement the stretching modes from the 5% Bp PAA were too weak to see clearly on the PAA background, so a sample with 18% Bp PAA was employed. As seen in

Figure 4, the benzophenone carbonyl bands at 1600.31 and the peaks between 1256-1318 cm^{-1} decrease with irradiation while the ester C=O mode at 1729 cm^{-1} remains constant, showing the rest of the polymer is unaffected by the UV.

Variation in mechanical properties

The apparent modulus of PEI(PAH/PAABp)$_{15}$ (317 nm wet thickness) varied over a wide range: 16 MPa up to 350 MPa after 100 min of irradiation (see Figure 5). The first 10 sec of irradiation yielded the largest jump in modulus as benzophenone molecules were fully available. As the irradiation time increased, the crosslinking density increased up to a maximum of 80%. Note that modulus measurements with nanoindentation have better precision than accuracy, but while the absolute value of E_a is model-dependent we are confident we can compare relative values here and with prior work, taken with the same apparatus. The starting (uncrosslinked) modulus of 16 MPa is greater than the starting modulus (6 Mpa) of thermal crosslinked PAH/PAA multilayers we reported.[33] The thermally crosslinked systems went up to 8 GPa at maximum crosslinking,[33] a range which is higher than obtained here by photocrosslinking, due to more extensive (close to 100%) crosslinking in the former system and the fact that not all photogenerated radicals will form a crosslink on a different chain. For comparison to other systems, that the modulus on chemical crosslinking of PLL and HA increased from 12 KPa to 450 KPa,[31] again in this case all amines and carboxylic acids are involved in the formation of amide bond. In comparison to other groups using photocrosslinking on PEMUS, Vazquez et al.,[18] who prepared a hyaluronan (HA) polyanion grafted with different densities of photocrosslinkable vinyl benzene, obtained a modulus range from about 35 KPa at 14 % grafted degree to about 140 KPa at maximum grafting of 37% after which the polyanion was no longer soluble. Our system had a 22-fold increase in modulus with 5% grafting degree of benzophenone on PAA. To extend the range, we prepared a PAA grafted with 18% bp where apparent modulus values up to 5 GPa at 50% crosslinking density (data not shown) were obtained. Thus, a wide range of modulus is available with the PAABp system. The morphology of PAH/PAABp multilayer before and after crosslinking was studied using AFM to check for structural changes. PEI(PAH/PAABp)$_{15}$ was imaged at 0 and 100 mins irradiation time (Figure S7). RMS surface roughness after photocrosslinking remained constant at about 7 nm.

Swelling of polymers by solvents is typically decreased by crosslinking. Dry and wet (Tris buffer, pH=7.4 and 0.15 M NaCl) thicknesses of a PEI(PAH/PAABp)$_{15}$ film were measured with AFM scanning over a scratch. Films swelled by 29% on immersion in the buffer (i.e. the hydrophobicity index was 1.29). Interestingly, the percent swelling was not affected by crosslinking (within error, 29 +/-5%). This could be because the films are already heavily crosslinked by ion pairing.

Contact angle measurements

Since a (photo) chemical reaction is occurring during crosslinking, we were interested in the effect on surface properties. Specifically, as with our prior PAH/PAA (thermal) crosslinking work,[33] we were interested in the response of mammalian cells cultured onto PEMUs of defined stiffness. Ideally, to explore the effect of substrate stiffness, the mechanical properties of a crosslinked PEMU should vary while the surface chemistry remains constant. For example, a PLL/HA multilayer showed significant changes in contact angle (wettability)[58] after chemical crosslinking with EDC/NHS. One of the benefits of employing a crosslinking strategy that does not change the net charge of a PEMU is that the ion content in the bulk and at the surface will also remain unchanged.

Contact angles for PAH or PAABp terminated PEMUs were followed as a function of crosslinking as shown in Figure 6. Small changes in surface wetting were observed on crosslinking, but overall the films appeared to preserve their contact angles over a wide range of crosslinking. Contact angles for PAH terminated PEMUS are about 35°, similar to those observed by Yoo et al.[59] for PAH/PAA films, whereas the PAABp terminated layers had contact angles of about 50°, much higher than observed for PAH/PAA, probably due to the hydrophobic Bp moiety.

Permeability of KI as a function of crosslinking

The permeability of PAH/PAA to various ions was studied by Harris et al.[14] under extremes of thermal crosslinking (i.e. "crosslinked" or "uncrosslinked"). In the present work the permeability of PAH/PAABp multilayers to iodide ion was evaluated for carefully controlled levels of crosslinking (i.e. irradiation time). Permeabilities were measured by the rate of electrochemical oxidation for PEMUs deposited on rotating platinum disc electrodes (RDE). All other parameters were kept constant: the salt concentration was 0.15 M the potassium iodide was 1 mM, and the rotation rate of the electrode was 1000 rpm. The final layer, and thus the final charge, was positive to remove the effect of charge repulsion. The ion flux is given directly by the electrochemical current. For a bare electrode the limiting current is given by the Levich equation.[49]

$$i_{lev} = 0.620 nFAD_{aq}^{2/3}\omega^{1/2}\upsilon^{-1/6}C_{aq} \tag{7}$$

where n is the number of electrons transferred, F is Faraday's constant (96 490 C mol-1). D_{aq} (cm^2 s^{-1}) is the solution diffusion coefficient of the electroactive species, υ is the kinematic viscosity, C_{aq} is the solution concentration, ω is the angular velocity (rad s^{-1}), and A is the electrode area.

The theory of current-voltage responses for membranes on RDEs was developed by Gough and Leypoldt,[60] and applied by Ikeda et al. to study the permeation of electroactive solutes through ultrathin films on RDEs.[61] A PEMU coating the electrode decreases the limiting current, i_l, as a result of the increasing resistance to mass transfer, as given in Equation 8.[61]

$$\frac{1}{i_l} = \frac{1}{i_m} + \frac{1}{i_{lev}} \tag{8}$$

where i_m is the current limited by permeation through the membrane (membrane current). As seen in Figure 7, the current decreased at different irradiation times. This decrease in current could be a result of various factors. First, crosslinking probably makes the PEMU less hydrated, as is usually seen with water-swollen gels.[62] Second, the material is likely to be less dopable by ions in solution, including iodide and chloride, yielding fewer iodide ions in the film and fewer charge carrier sites.[29] Third, the photocrosslinking network, which cannot be broken, probably offers an additional physical barrier to ion transport. A decrease in ion permeability for a photocrosslinked multilayer was also seen by Kang et al.[25] using cyclic voltammograms. Others controlled the permeability of polyelectrolyte multilayer by changing the salt concentration where at higher salt concentration the multilayer is swelled and is less resistant to ion transport.[49] Here we provide a system with controllable permeability by grafting the PAA with 5 % benzophenone. Permeability control without changing the charge content of the multilayer; is significant because charge content controls permeability.

Conclusions

The multilayers examined here exhibited a smooth increase in modulus, with a concomitant decrease in permeability, on photocrosslinking. Transmission FTIR supported the literature mechanism for benzophenone crosslinking. Each of the methods available for crosslinking PEMUS – photochemistry, thermal and chemical reactions – has its own advantages and disadvantages. Using the thickness data in Figure 1 and the absorption data in Figure 3, PEMUs up to about a micrometer thick are suitable for photocrosslinking. Thermal and chemical crosslinking may be performed on thicker articles, but lack the potentially high spatial resolution of photocrosslinking. In addition, photocrosslinking is least likely to perturb the chemical structure, especially the charge content, of multilayers and may be carried out on capsules or planar surfaces. Polyelectrolyte complexes of any morphology are heavily crosslinked by ion pairing. The addition of chemical crosslinks produces an interesting "dual crosslinked" material, where only one type of crosslink may be broken by increasing ionic strength.

Supplementary Material

Refer to Web version on PubMed Central for supplementary material.

Acknowledgments

References

1. Boudou T, Crouzier T, Ren K, Blin G, Picart C. Adv Mater. 2010; 22:441–467. [PubMed: 20217734]

2. Engler AJ, Griffin MA, Sen S, Boennemann CG, Sweeney HL, Discher DE. J. Cell Biol. 2004; 166:877–887. [PubMed: 15364962]

3. Discher DE, Janmey P, Wang Y.-l. Science. 2005; 310:1139–1143. [PubMed: 16293750]

4. Isenberg BC, Di Milla PA, Walker M, Kim S, Wong JY. Biophys. J. 2009; 97:1313–1322. [PubMed: 19720019]

5. Pelham RJ Jr. Wang Y-L. Biol. Bull. 1998; 194:348–350. [PubMed: 11536880]

6. Wong JY, Velasco A, Rajagopalan P, Pham Q. Langmuir. 2003; 19:1908–1913.

7. Lo C-M, Wang H-B, Dembo M, Wang Y-L. Biophys. J. 2000; 79:144–152. [PubMed: 10866943]

8. Flanagan Lisa A, Ju Y-E, Marg B, Osterfield M, Janmey Paul A. Neuroreport. 2002; 13:2411–2415. [PubMed: 12499839]

9. Engler AJ, Sen S, Sweeney HL, Discher DE. Cell. 2006; 126:677–689. [PubMed: 16923388]

10. Maloney JM, Walton EB, Bruce CM, Van Vliet KJ. Phys. Rev. E. 2008; 78:041923/041921–041923/041915.

11. Mehrotra S, Hunley SC, Pawelec KM, Zhang L, Lee I, Baek S, Chan C. Langmuir. 2010; 26:12794–12802. [PubMed: 20604583]

12. Jaber JA, Schlenoff JB. J. Am. Chem. Soc. 2006; 128:2940–2947. [PubMed: 16506773]

13. Bruening ML, Sullivan DM. Chem.--Eur. J. 2002; 8:3832–3837.

14. Harris JJ, DeRose PM, Bruening ML. J. Am. Chem. Soc. 1999; 121:1978–1979.

15. Picart C, Senger B, Sengupta K, Dubreuil F, Fery A. Colloids Surf., A. 2007; 303:30–36.

16. Zhu H, Ji J, Tan Q, Barbosa MA, Shen J. Biomacromolecules. 2003; 4:378–386. [PubMed: 12625735]

17. Ducker RE, Montague MT, Leggett GJ. Biointerphases. 2008; 3:59–65. [PubMed: 20408701]

18. Pozos Vazquez C, Boudou T, Dulong V, Nicolas C, Picart C, Glinel K. Langmuir. 2009; 25:3556–3563. [PubMed: 19275180]

19. Nguyen KT, West JL. Biomaterials. 2002; 23:4307–4314. [PubMed: 12219820]

20. Park M-K, Deng S, Advincula RC. J. Am. Chem. Soc. 2004; 126:13723–13731. [PubMed: 15493931]

21. Olugebefola SC, Kuhlman WA, Rubner MF, Mayes AM. Langmuir. 2008; 24:5172–5178. [PubMed: 18318557]

22. Olugebefola SC, Ryu S-W, Nolte AJ, Rubner MF, Mayes AM. Langmuir. 2006; 22:5958–5962. [PubMed: 16768536]

23. Park M-K, Deng S, Advincula RC. Langmuir. 2005; 21:5272–5277. [PubMed: 15924449]

24. Sun J, Wu T, Sun Y, Wang Z, Xi Z, Shen J, Cao W. Chem. Commun. 1998:1853–1854.

25. Kang E-H, Liu X, Sun J, Shen J. Langmuir. 2006; 22:7894–7901. [PubMed: 16922580]

26. Gauczinski J, Liu Z, Zhang X, Schönhoff M. Langmuir. 2010; 26:10122–10128. [PubMed: 20334393]

27. Dai J, Jensen AW, Mohanty DK, Erndt J, Bruening ML. Langmuir. 2001; 17:931–937.

28. Harris JJ, Stair JL, Bruening ML. Chem. Mater. 2000; 12:1941–1946.

29. Farhat TR, Schlenoff JB. J. Am. Chem. Soc. 2003; 125:4627–4636. [PubMed: 12683835]

30. Richert L, Boulmedais F, Lavalle P, Mutterer J, Ferreux E, Decher G, Schaaf P, Voegel J-C, Picart C. Biomacromolecules. 2004; 5:284–294. [PubMed: 15002986]

31. Schneider A, Francius G, Obeid R, Schwinte P, Hemmerle J, Frisch B, Schaaf P, Voegel J-C, Senger B, Picart C. Langmuir. 2006; 22:1193–1200. [PubMed: 16430283]

32. Vinckier A, Semenza G. FEBS Lett. 1998; 430:12–16. [PubMed: 9678586]

33. Moussallem MD, Olenych SG, Scott SL, Keller TCS, Schlenoff JB. Biomacromolecules. 2009; 10:3062–3068. [PubMed: 19817347]

34. Pharr GM, Oliver WC, Brotzen FR. J. Mater. Res. 1992; 7:613–617.

35. Domke J, Radmacher M. Langmuir. 1998; 14:3320–3325.

36. Picart C, Lavalle P, Hubert P, Cuisinier FJG, Decher G, Schaaf P, Voegel JC. Langmuir. 2001; 17:7414–7424.

37. Jaber JA, Schlenoff JB. Chem. Mater. 2006; 18:5768–5773.

38. Akhremitchev BB, Walker GC. Langmuir. 1999; 15:5630–5634.

39. Sneddon IN. Int. J. Eng. Sci. 1965; 3:47–57.

40. Korsunsky AM. J. Strain Anal. Eng. 2001; 36:391–400.

41. Dubas ST, Schlenoff JB. Langmuir. 2001; 17:7725–7727.

42. Thompson MT, Berg MC, Tobias IS, Rubner MF, Van Vliet KJ. Biomaterials. 2005; 26:6836–6845. [PubMed: 15972236]

43. Dubas ST, Schlenoff JB. Macromolecules. 2001; 34:3736–3740.

44. Sukhishvili SA, Granick SJ. Am. Chem. Soc. 2000; 122:9550–9551.

45. Schlenoff JB, Rmaile AH, Bucur CB. J. Am. Chem. Soc. 2008; 130:13589–13597. [PubMed: 18798621]

46. Wong JE, Rehfeldt F, Haenni P, Tanaka M, Klitzing R. v. Macromolecules. 2004; 37:7285–7289.

47. Blacklock J, Vetter A, Lankenau A, Oupicky D, Möhwald H. Biomaterials. 2010; 31:7167–7174. [PubMed: 20580430]

48. Lvov, Y. Protein Architecture: Interfacing Molecular Assemblies and Immobilization Biotechnology. Lvov, Y.; Möhwald, H., editors. M. Dekker; New York: 2000. Chapter. 6

49. Farhat TR, Schlenoff JB. Langmuir. 2001; 17:1184–1192.

50. McCormick M, Smith RN, Graf R, Barrett CJ, Reven L, Spiess HW. Macromolecules. 2003; 36:3616–3625.

51. Schwarz B, Schönhoff M. Langmuir. 2002; 18:2964–2966.

52. Chen J, Huang L, Ying L, Luo G, Zhao X, Cao W. Langmuir. 1999; 15:7208–7212.

53. Wu G, Shi F, Wang Z, Liu Z, Zhang X. Langmuir. 2009; 25:2949–2955. [PubMed: 19437767]

54. Prucker O, Naumann CA, Rühe J, Knoll W, Frank CW. J. Am. Chem. Soc. 1999; 121:8766–8770.

55. Wagner P, Park BS. Org. Photochem. 1991; 11:227–366.

56. Timpe H-J. Polymer Photochemistry and Photocrosslinking. Desk Reference of Functional Polymers. 1997

57. Turro NJ. Modern Molecular Photochemistry. 1978

58. Ren K, Crouzier T, Roy C, Picart C. Adv. Funct. Mater. 2008; 18:1378–1389. [PubMed: 18841249]

59. Yoo D, Shiratori SS, Rubner MF. Macromolecules. 1998; 31:4309–4318.

60. Gough DA, Leypoldt JK. Anal. Chem. 1979; 51:439–444.

61. Ikeda T, Schmehl R, Denisevich P, Willman K, Murray RW. J. Am. Chem. Soc. 1982; 104:2683–2691.

62. Hirotsu S. Macromolecules. 2004; 37:3415–3424.
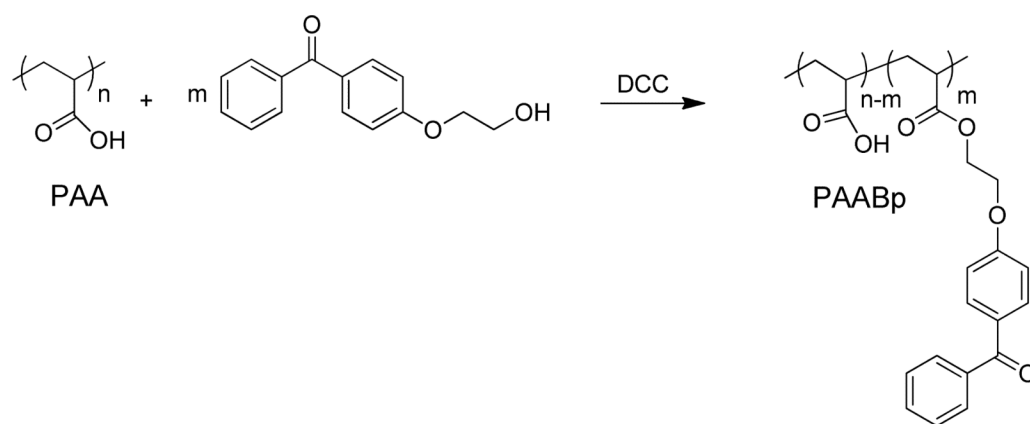
Scheme 1.
Grafting procedure of PAA with 4-(2-hydroxyethoxy)benzophenone. m = 0.05n
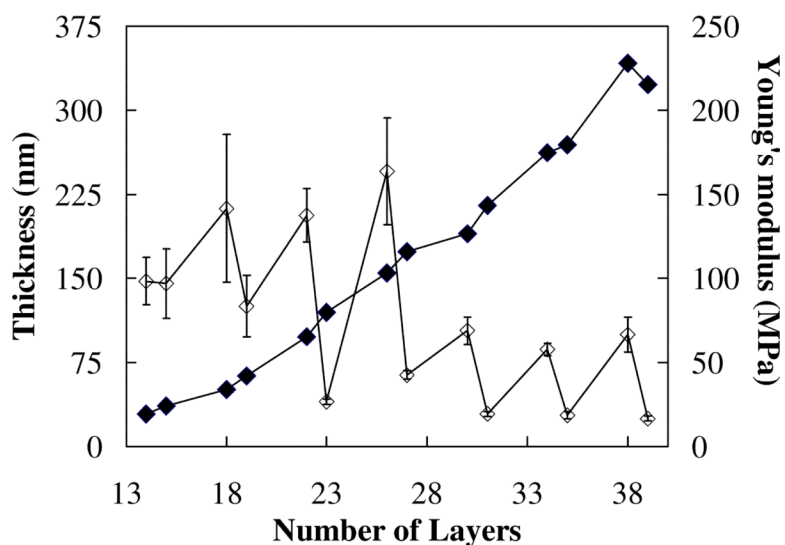
Figure 1.
◆ Dry film thickness as a function of the number of layers for PAH/PAA multilayer buildup. ◇; variation of apparent Young's modulus as a function of film thickness and the final layer. The modulus was obtained by in situ AFM force curves measured in Tris buffer at pH= 7.4 and 0.15 M NaCl. The last point in the thickness series has a greater error.
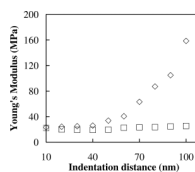
Figure 2.
Dependence on apparent modulus as a function of indentation distance for a multilayer of (□) 31 layers; and (◇) 23 layers of PAH/PAA. At higher indentations the tip "feels" the substrate and the apparent modulus increase significantly. All force curve measurements were performed at room temperature while the multilayer is immersed in Tris buffer (pH= 7.4, 0.15 M NaCl).
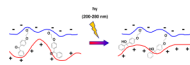
Scheme 2.
Mechanism of benzophenone photo-crosslinking. Occurs randomly with both negative and positive chains.
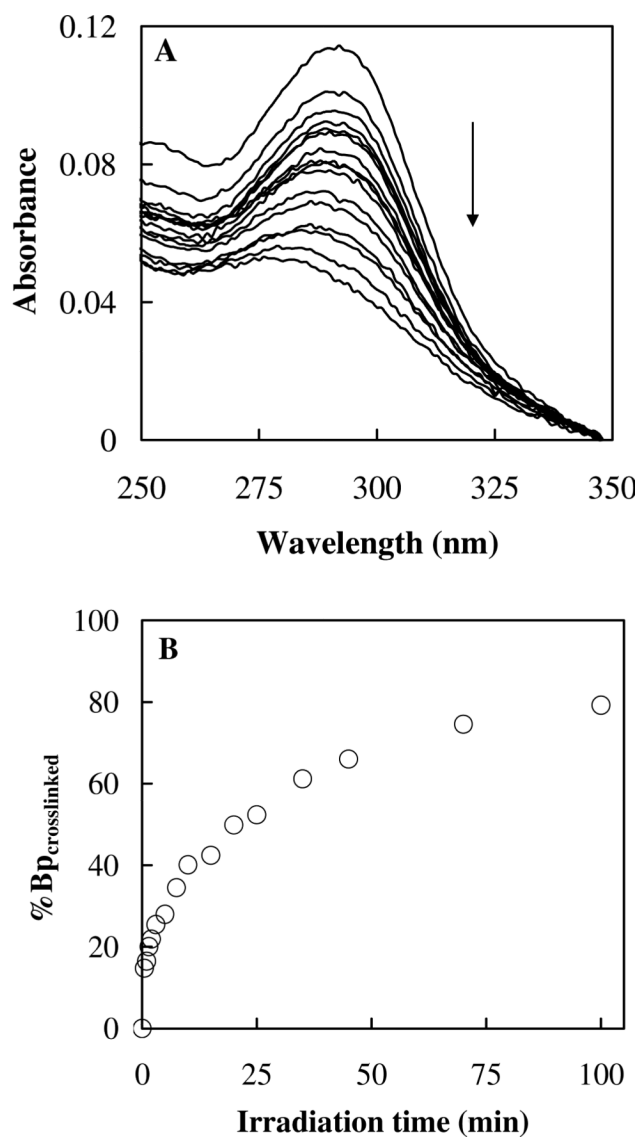
Figure 3.
Shows the efficiency of crosslinking of PEI(PAH/PAABp)$_{15}$ built on fused silica slide at different irradiation times. (A) UV-Visible spectra of Bp, the arrow indicates the decrease in Bp peak before and after 0.5, 1, 1.5, 2, 3, 5, 7.5, 10, 15, 20, 25, 35, 45, 70, and 100 minutes of irradiation. (B) The increase in percentage of crosslinked benzphenone at the different irradiation times obtained from Equation 3.
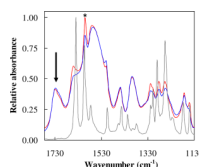
Figure 4.
FTIR spectra of PEI(PAABp/PAH)$_{90}$ before (red) and after (blue) 100 min irradiation, and of 4-(2-hydroxyethoxy)benzophenone (grey). The peak at 1729 cm^{-1}, indicated by an arrow, is from the ester bond between PAA and 4-(2-hydroxyethoxy)benzophenone. The peak corresponding to the diarylketone at 1600 cm^{-1}, indicated by an asterisk, decreased significantly after irradiation. In this PEMU the PAABp was 18% substituted by Bp. FTIR spectra of PAA/PAH and PAABP/PAH, shown for comparison in Supporting Information (see Figure S8), confirm that the 1729 cm^{-1} band is from the ester link.
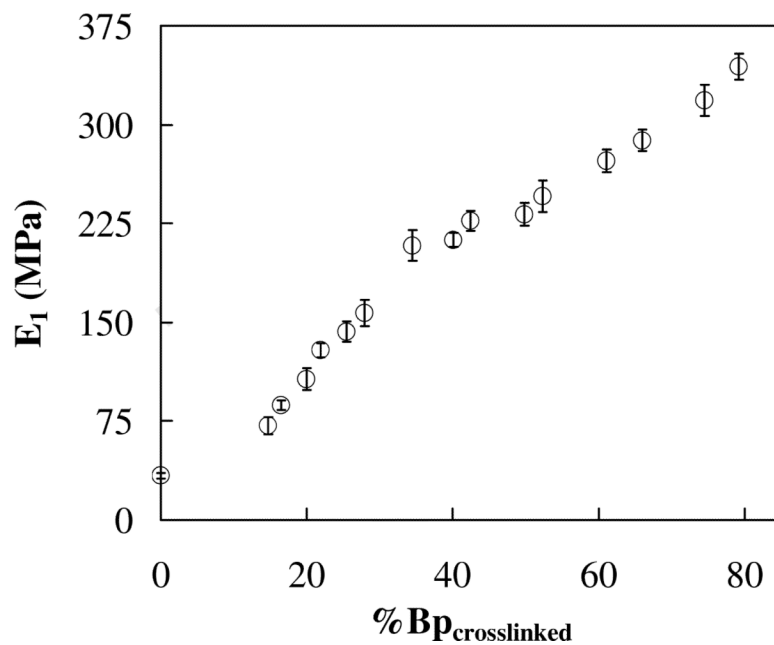
Figure 5.
Variation of apparent modulus of PEI(PAH/PAABp)$_{15}$ multilayer obtained by force curve measurements using atomic force microscope as a function of crosslink density. The measurements were conducted under wet conditions where the multilayer was immersed in tris buffer at pH= 7.4 with 0.15 M NaCl.
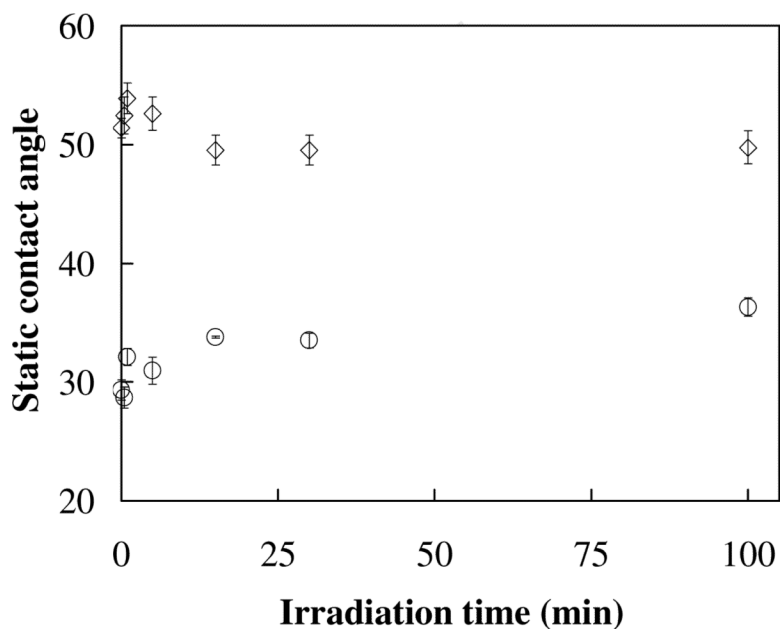
Figure 6.
The change in static contact angle of PAH/PAAbp 30 layers (◇), and 31 layers (o) as function of irradiation time.
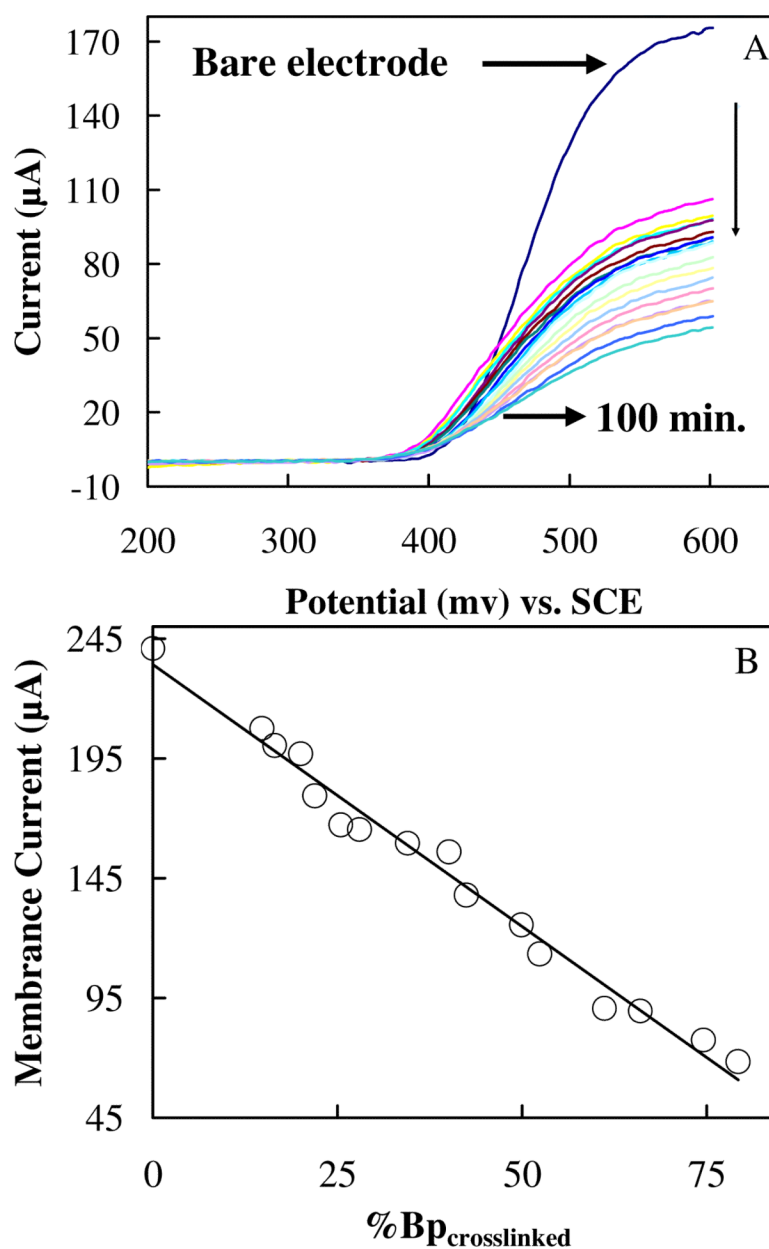
Figure 7.
(A) Linear scan voltammograms of a rotating disc electrode. Decrease in current is a result of decreased transport of KI through a PEI(PAH/PAABp)$_{15}$ multilayer built on a platinum electrode before and after 0.5, 1, 1.5, 2, 3, 5, 7.5, 10, 15, 20, 25, 30, 35, 45, 70, and 100 mins of irradiation. The highest current is for the bare electrode. (B) membrane current as a function of % of crosslinking. All measurements were performed in 0.15 M NaCl and 1 mM KI at 1000 rpm.